Journal of Catalysis 287 (2012) 161–169

Contents lists available at SciVerse ScienceDirect

Journal of Catalysis

journal homepage: www.elsevier.com/locate/jcat

Hydrodesulfurization of dibenzothiophene and its hydrogenated intermediates over bulk MoP

Jin Bai [a], Xiang Li [a,b,*], Anjie Wang [a,b], Roel Prins [c], Yao Wang [b]

[a] State Key Laboratory of Fine Chemicals, School of Chemical Engineering, Dalian University of Technology, No. 2 Linggong Road, Dalian 116024, PR China
[b] Liaoning Key Laboratory of Petrochemical Technology and Equipments, Dalian University of Technology, No. 2 Linggong Road, Dalian 116024, PR China
[c] Institute of Chemical and Bioengineering, ETH Zurich, 8093 Zurich, Switzerland

ARTICLE INFO

Article history:
Received 12 October 2011
Revised 17 December 2011
Accepted 21 December 2011
Available online 31 January 2012

Keywords:
Hydrodesulfurization
Dibenzothiophene
Hydrogenated intermediates
Molybdenum phosphide
Piperidine

ABSTRACT

The hydrodesulfurization (HDS) of dibenzothiophene (DBT) and its hydrogenated intermediates 1,2,3,4-tetrahydro-dibenzothiophene (TH-DBT) and 1,2,3,4,4a,9b-hexahydro-dibenzothiophene (HH-DBT) over a bulk MoP catalyst was studied at 340 °C and 4 MPa both in the presence and absence of piperidine. The results indicated that sulfur was incorporated on the surface of MoP during HDS reactions, probably leading to the formation of new active sites, which possessed higher direct desulfurization (DDS) activity than the fresh MoP. The hydrogenation pathway and DDS pathway played an equally important role in the HDS of DBT. The desulfurization of TH-DBT was much faster than that of DBT, whereas HH-DBT mainly desulfurized by dehydrogenation to TH-DBT and subsequent desulfurization of TH-DBT. Piperidine decreased the rates of all reactions, but that of hydrogenation more than of desulfurization. It not only competed with the sulfur-containing molecules for adsorption on the active sites but also slowed down the sulfidation of MoP surface.

1. Introduction

Transition-metal phosphides (e.g., MoP, WP, Co_2P, CoP, Ni_2P) [1–6] and noble-metal phosphides [7,8] have attracted increasing attention as a new family of non-sulfidic hydrodesulfurization (HDS) catalysts, due to their high activity and stability under HDS conditions. In particular, molybdenum phosphide and nickel phosphide have shown promise, with activities similar to or higher than those of sulfide-based catalysts [9]. Ni_2P exhibited excellent activity in hydroprocessing [10,11]. The overall activity of the transition-metal phosphides in the simultaneous HDS of dibenzothiophene (DBT) and hydrodenitrogenation (HDN) of quinoline was in the order of Fe_2P < CoP < MoP < WP < Ni_2P [2,10]. MoP possessed a moderate activity for simultaneous HDN and HDS, but its intrinsic activity for the HDN of *o*-propylaniline was six times higher than that of Mo edge atoms in γ-Al_2O_3-supported MoS_2 [12]. Of the Co_2P, Ni_2P, MoP, WP, CoMoP, and NiMoP catalysts, MoP is intrinsically the most active HDN catalyst [12,13]. For a further development of high-performance transition-metal phosphide HDS catalysts, an in-depth understanding of the HDS reaction mechanisms and kinetics of sulfur-containing molecules over this new family of HDS catalysts is needed.

DBT and its alkylated derivates, especially those alkylated at the 4 and 6 positions (4,6-dimethyldibenzothiophene, 4,6-DMDBT), are the most refractory sulfur-containing compounds in gas oil [14–17]. Consequently, they are often chosen as model molecules in HDS studies. HDS studies over transition-metal phosphides have been carried out mainly with DBT and 4,6-DMDBT, even though the HDS reaction networks of these polyaromatic sulfur-containing molecules are complex. DBT and alkyl-substituted DBT undergo HDS by two parallel pathways: direct desulfurization (DDS) and hydrogenation (HYD) [18,19]. DDS leads to the formation of biphenyls, while HYD yields tetrahydro (TH), hexahydro (HH), and dodecahydro (DH) sulfur-containing intermediates, which are desulfurized to cyclohexylbenzenes and bicyclohexyls [19]. Therefore, the HDS reactions of both the parent sulfur-containing molecules and their hydrogenated intermediates should be investigated to gain sufficient information on the removal of the sulfur atoms over transition-metal phosphides. Recently, the synthesis of large amounts of the tetrahydro and hexahydro intermediates of DBT and 4,6-DMDBT has made such investigations possible [20–22].

Previously, we studied the HDS of DBT and its two hydrogenated intermediates 1,2,3,4-TH-DBT (TH-DBT) and 1,2,3,4,4a, 9b-HH-DBT (HH-DBT) over bulk Ni_2P [23] and found that the first C–S bond breakage of HH-DBT over Ni_2P occurs through an β-elimination mechanism in which the hydrogen attached to carbon atom C(4) is involved. This indicates that studies of the HDS of the polyaromatic sulfur-containing molecules and their hydrogenated intermediates over the novel transition-metal phosphide

* Corresponding author. Address: School of Chemical Engineering, Dalian University of Technology, Dalian 116024, PR China. Fax: +86 411 84986121.
E-mail address: lixiang@dlut.edu.cn (X. Li).

0021-9517/$ - see front matter © 2011 Elsevier Inc. All rights reserved.
doi:10.1016/j.jcat.2011.12.018

HDS catalysts will provide new insight into questions about reaction mechanisms and the structure and activity relationships of the HDS catalysts. Therefore, we studied the HDS of DBT, TH-DBT, and HH-DBT over the other important transition-metal phosphide, MoP, in the present work.

2. Experimental methods

2.1. Preparation of DBT and its hydrogenated intermediates

DBT was synthesized according to a method described in the literature [24]. TH-DBT was synthesized in two steps according to the method of DiCesare et al. [25], except that 2-bromocyclohexanone instead of 2-chlorocyclohexanone was used in the first step. In the second step, 2-thiophenoxy-cyclohexanone, which was obtained from the reaction of 2-bromocyclohexanone with thiophenol, was heated with polyphosphoric acid to form TH-DBT. HH-DBT was produced by hydrogenation of TH-DBT with zinc and trifluoroacetic acid at room temperature [18].

2.2. Preparation of MoP catalyst precursor

Molybdenum phosphate was prepared by dropwise adding an aqueous solution of 3.90 g $(NH_4)_6Mo_7O_{24}{\cdot}H_2O$ in 15 mL deionized water to a solution of 3.0 g $(NH_4)_2HPO_4$ in 10 mL deionized water under stirring. The resulting precipitate was stirred while the water was evaporated to obtain a solid product, which was dried at 120 °C for 12 h and calcined at 500 °C for 3 h to obtain the final oxidic precursor having a Mo/P molar ratio of 1.

2.3. HDS activity measurement

The catalytic reactions were carried out in a stainless-steel tubular reactor (8.0 mm i.d.). The precursor was pelleted, crushed, and sieved to 20 to 30 mesh. A total of 0.10 g precursor was used for each run. Prior to HDS reaction, the precursor was transformed into bulk MoP by in situ H_2 temperature-programmed reduction [26]. It was heated from room temperature to 550 °C at 5 °C/min in H_2 (150 mL/min), then to 650 °C at 1 °C/min, and finally kept at 650 °C for 2 h.

After the precursor had been converted into molybdenum phosphide, the reactor was cooled to the reaction temperature of 340 °C, the total pressure was increased to 4 MPa, and the gas-phase feed, consisting of 1 kPa reactant (DBT, TH-DBT, or HH-DBT), 165 kPa decalin (as solvent), 0 or 0.25 kPa piperidine (Pi, Acros), and about 3.8 MPa H_2, was fed to the reactor. Each HDS reaction run was divided into four consecutive stages: high weight time → low weight time → high weight time → low weight time → high weight time. After two stages, the HDS performance of MoP became stable in most cases. Therefore, only the yields and product selectivities of the first two stages will be shown. Weight time [27] was defined as $\tau = w_{cat}/n_{feed}$, where w_{cat} denotes the catalyst weight and n_{feed} the total molar flow to the reactor (1 g min/mol = 0.15 g h/l). The weight time was changed by varying the flow rates of the liquid and gas, while keeping their ratio constant. The reaction products were analyzed off-line by an Agilent-6890 N gas chromatograph equipped with a HP-5 column and a flame ionization detector. A DB-VAX column (J&W Scientific) was used to quantify the 1-cyclohexen-1-yl-benzene (CHEB-1), 2-cyclohexen-1-yl-benzene (CHEB-2), and 3-cyclohexen-1-yl-benzene (CHEB-3) present in the HDS products.

2.4. Characterization

XRD pattern of the MoP catalyst was measured on a Rigaku D/Max 2400 diffractometer with nickel-filtered Cu Kα radiation at 40 kV and 100 mA. A nitrogen adsorption measurement was performed on a Micromeritics Tristar II 3020 analyzer. The quantitative elemental analysis of the bulk MoP before and after HDS reaction was performed using an X-ray fluorescence (XRF) analyzer (RSR 3400 X). The surface of the spent MoP was analyzed by X-ray photoelectron spectroscopy (XPS) with a MultiLab 2000 X-ray photoelectron spectrometer, using an Mg Kα source. For the individual energy regions, a pass energy of 20 eV was used. All binding energies were referenced to the C 1s peak at 284.6 eV. Before the characterization, the fresh MoP sample was prepared according to the same reduction conditions as used in the in situ reduction, followed by passivation with 0.5% (volume) O_2 in Ar. The spent MoP was used directly for the further XRF and XPS measurements after being dried under the reaction temperature (340 °C) with a N_2 flow.

CO adsorption was measured using pulsed chemisorption as described in the literature [28]. About 0.2 g passivated, air-exposed MoP sample was re-reduced in a H_2 flow to remove the passivation layer (80 mL/min flow rate, heating from 25 to 500 °C at a rate of 10 °C/min, and then holding at the final temperature for 1 h). The reactor was then cooled to 30 °C in a flow of H_2. An Ar flow at 80 mL/min was used to flush the catalyst for 30 min to achieve an adsorbate-free, reduced catalyst surface. After pretreatment, 1.25 mL pulses of 1% CO in Ar were injected into a flow of Ar (80 mL/min), and the CO uptake was measured using a TCD detector. CO pulses were repeatedly injected until the response from the detector showed no further CO uptake.

3. Results

3.1. Characterization

The XRD pattern of the MoP catalyst indicated that molybdenum phosphide had formed during reduction in the oxidic precursor (Fig. 1). The crystallite size of the prepared MoP was estimated from the XRD line width to be 17 nm. The MoP had a low surface area (3.8 m^2/g) and a CO uptake of 2.2 μmol/g. These data are close to those reported previously for unsupported MoP [13,28]. The P/Mo atomic ratio of the fresh MoP determined by XRF was 0.92/1. This value is very close to the nominal one. No sulfur was detected in the fresh MoP. On the other hand, about 1.5 wt.% sulfur (based on SO_3) was found in the spent MoP, and the atomic ratio of S/P/Mo was calculated to be 0.045/1.03/1.

The XPS spectra in the Mo 3d, P 2p, and S 2p regions for the spent MoP are shown in Fig. 2. Mo 3d spectrum consists of two split peaks due to spin and orbit interaction, with a separation of 3.2 eV and an intensity ratio of 1.5 [29]. The assignment of the

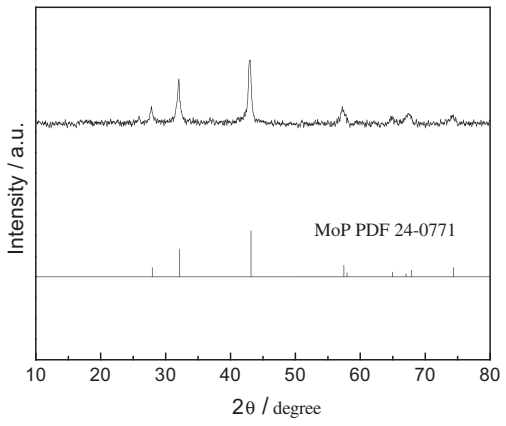

Fig. 1. XRD pattern of the fresh MoP and reference PDF 24-0771.

oxidation states of different Mo oxides is based on the Mo ($3d_{3/2,5/2}$) spin and orbit components. These energies are at 235.85 and 232.65 eV for MoO_3, 234.9 and 231.7 eV for Mo_2O_5, 232.3 and 229.1 eV for MoO_2, and 230.85 and 227.7 eV for Mo(0) [30]. For the spent MoP, the doublet with a separation (3.2 eV) identically to the theoretical one located at 228.1 and 231.3 eV can be attributed to $Mo^{\delta+}$ species ($0 < \delta \leqslant 4$), which are generally related to the molybdenum species in MoP [28,31]. The predominant P species on the surface of the catalyst with a P $2p_{3/2}$ binding energy of 129.5 eV can be assigned to P bonded to Mo (i.e., phosphide), while the small peak at 134.3 eV was due to surface PO_4^{3-} species probably produced when the catalyst was exposed to air [31]. The S 2p peak observed in the spectrum of the spent MoP can be deconvoluted into two Gaussian peaks, located at 161.5 and 162.5 eV, assigned to sulfide species (S^{2-}) and the thiolate-type sulfur [32], respectively. The surface S/P/Mo atomic ratio of the spent MoP estimated by XPS was 0.35/1.37/1. The surface S/Mo ratio (0.35) was almost eight times higher than the bulk value (0.045) measured by XRF, indicating S was mainly incorporated on the surface of MoP after the HDS reaction.

3.2. HDS of DBT

The products observed during the HDS of DBT over bulk MoP were BP, the product of the DDS pathway, TH-DBT and HH-DBT, the intermediates of the HYD pathway, and CHB and BCH, the final products of the HYD pathway. No DH-DBT and CHEBs were detected. In the first stage (high weight time → low weight time) of the HDS reaction, the DBT conversion was 53% at the start at τ = 1.5 g min/mol (solid line, Fig. 3A), higher than the conversion over bulk Ni_2P, which had a higher CO uptake (5.0 μmol/g) under the same conditions [23]. The yields of all products increased with weight time. BP was the most abundant product (solid line, Fig. 3A), with a yield of 22% at τ = 1.5 g min/mol. CHB was the second most abundant product, and its yield at τ = 1.5 g min/mol (19%) was close to that of BP. The selectivity to BP decreased from 57% at low weight time to 42% at high weight time, while the selectivities to CHB and BCH increased with weight time (solid lines, Fig. 4A). TH-DBT behaved as a primary product, because its selectivity decreased with weight time (solid line, Fig. 4A).

During the second stage of the HDS reaction (low weight time → high weight time), an increase in DBT conversion was observed. At τ = 1.5 g min/mol, the conversion of DBT increased to 68% (dashed line, Fig. 3A), mainly due to an increase in the BP yield. Only a small increase in the CHB yield was observed, while the yields of TH-DBT and HH-DBT decreased. As a consequence, the selectivities to the products of the HYD pathway (TH-DBT, HH-DBT, CHB, and BCH) decreased, while the selectivity to BP increased in the second stage (dashed lines, Fig. 4A). The selectivity of BP was almost constant with weight time during the second stage (dashed line, Fig. 4A). It was less than 60%, indicating that both HYD and DDS pathways play an important role in the DBT HDS catalyzed by the bulk MoP.

Pi had a negative influence on the conversion of DBT, as observed before over bulk Ni_2P [23]. At 0.25 kPa Pi, the DBT conversion decreased to 23% at τ = 1.5 g min/mol (solid line, Fig. 3B). The yields of all products decreased in the presence of Pi, indicating that Pi inhibits both DDS and HYD pathways. The inhibition effect of Pi was stronger on the HYD pathway than on the DDS pathway, because the selectivity of BP was about 10 to 15% higher in the presence than in the absence of Pi (solid lines, Fig. 4A and B). Due to the drastic decrease in the yield of CHB in the presence of Pi, TH-DBT became the most abundant product in the HYD pathway at τ < 0.74 g min/mol (solid line, Fig. 4B). Similar to the

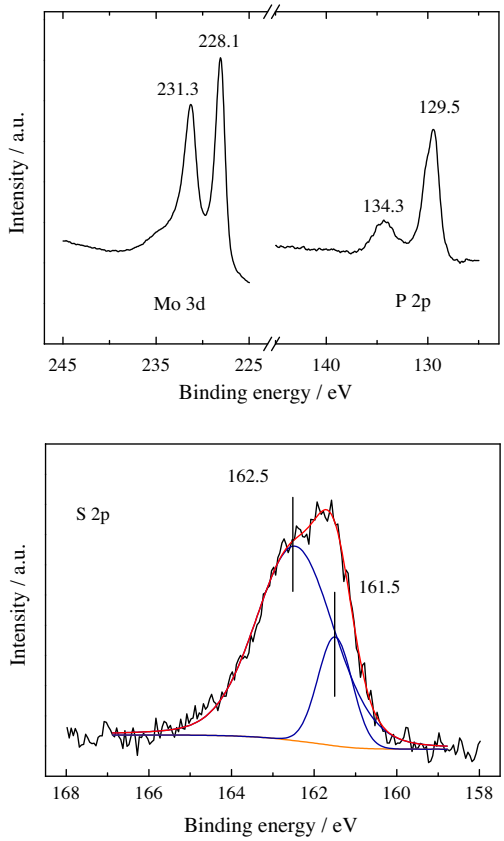

Fig. 2. XPS spectra of the spent MoP in Mo 3d, P 2p, and S 2p regions.

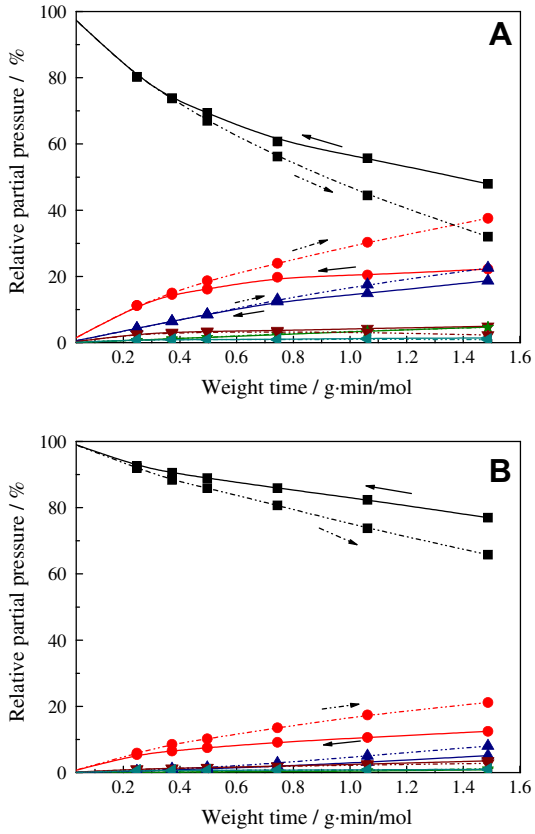

Fig. 3. Relative partial pressures of the reactant and products in the HDS of DBT over bulk MoP at 340 °C and 0 kPa Pi (A) and 0.25 kPa Pi (B) as a function of weight time. ● BP; ▲ CHB; ★ BCH; ▼ TH-DBT; ◄ HH-DBT; ■ DBT. The arrows indicate whether the weight time was increased or decreased.

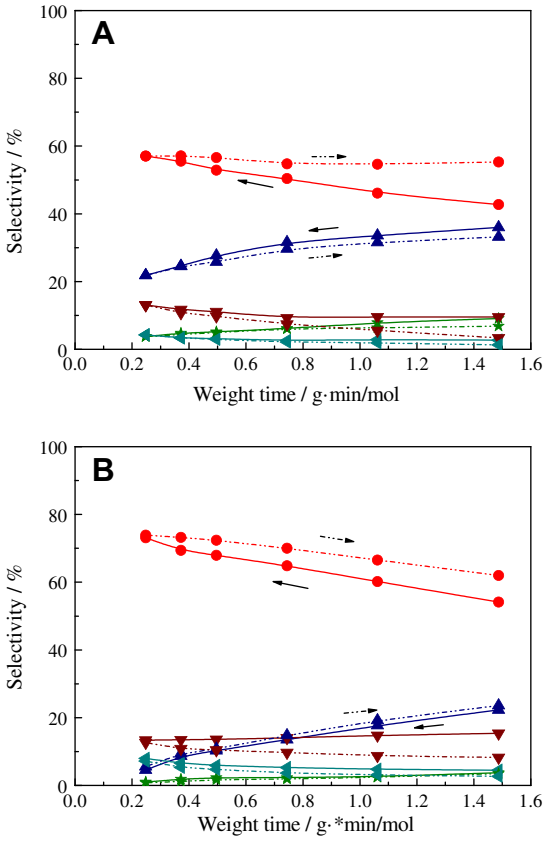

Fig. 4. Product selectivities in the HDS of DBT over bulk MoP at 340 °C and 0 kPa Pi (A) and 0.25 kPa Pi (B) as a function of weight time. ● BP; ▲ CHB; ★ BCH; ▼ TH-DBT; ◄ HH-DBT. The arrows indicate whether the weight time was increased or decreased.

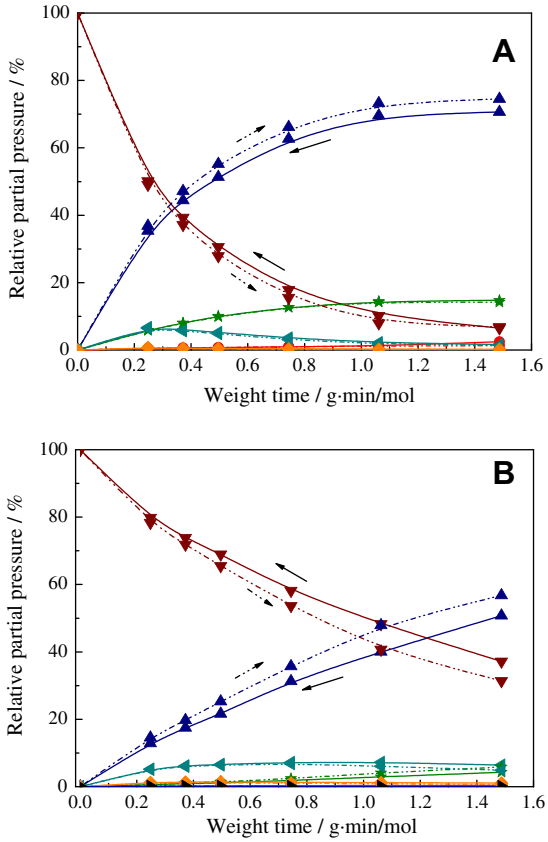

Fig. 5. Relative partial pressures of the reactant and products in the HDS of TH-DBT over bulk MoP at 340 °C and 0 kPa Pi (A) and 0.25 kPa Pi (B) as a function of weight time. ● BP; ▲ CHB; ★ BCH; ▼ TH-DBT; ◄ HH-DBT; ♦ CHEB-1; ▶ CHEB-3. The arrows indicate whether the weight time was increased or decreased.

observations in the absence of Pi, the DBT conversion as well as the yields of BP and CHB all increased during the second stage of HDS reaction in the presence of Pi, and the increase in the HDS activity was mainly due to the increase in the DDS pathway activity of MoP (dashed lines, Fig. 3B). This led to an increase in the BP selectivity, which still decreased with weight time even in the second stage of reaction (dashed lines, Fig. 4B).

3.3. HDS of TH-DBT

The reactivity of TH-DBT over bulk MoP was higher than that of DBT. Its conversion was 93% at the start at τ = 1.5 g min/mol (solid line, Fig. 5A). Five products, HH-DBT, CHB, BCH, CHEB-1, and a trace amount of BP, were observed in the absence of Pi. The yield of HH-DBT went through a maximum (solid line, Fig. 5A) while its selectivity decreased as a function of weight time (solid line, Fig. 6), demonstrating that HH-DBT is both the primary product and the desulfurization intermediate of the HDS of TH-DBT. TH-DBT and HH-DBT tended to equilibrium at high weight time. The yields of CHB and BCH increased with weight time, indicating that they were the final products of the HDS of TH-DBT. CHB was the main product, with a selectivity of about 73% at τ = 1.5 g min/mol (solid line, Fig. 6A). BCH was the second most abundant one and its yield reached 16% at τ = 1.5 g min/mol (solid line, Fig. 5A). The selectivities of CHB and BCH were nearly constant (Fig. 6A), suggesting that their further reactions were slow. In the absence of Pi, the HDS performance of MoP in the second stage of TH-DBT HDS reaction was almost identical to that in the first stage. Only a slight increase in the yield and selectivity of CHB and decrease in the HH-DBT formation were observed (dashed lines, Figs. 5A and 6A).

The conversion of TH-DBT was only 63% at τ = 1.5 g min/mol in the presence of 0.25 kPa Pi (solid line, Fig. 5B). The yields of all products were decreased by the addition of Pi. This inhibition effect was particularly pronounced for the formation of BCH, which was strongly suppressed by Pi (solid line, Fig. 5B). As a result, CHB was still the most abundant product during the HDS of TH-DBT, but HH-DBT became the second abundant product. At τ < 0.4 g min/mol, the selectivity of CHEB-1 was even higher than that of BCH (solid line, Fig. 6B). It decreased with weight time, indicating that CHEB-1 was a primary product of the HDS of TH-DBT. The selectivities of CHB and BCH increased with weight time in the presence of Pi, suggesting that these molecules are the final products of the HDS of TH-DBT. A trace amount of CHEB-3 was detected at τ < 0.5 g min/mol.

During the second stage of the HDS of TH-DBT in the presence of Pi, an increase in activity was observed. The conversion of TH-DBT increased from 63% in the first stage to 70% in the second stage at τ = 1.5 g min/mol (dashed line, Fig. 5B). The increase in conversion was mainly due to the increase in the yield of CHB, as evidenced by the increase in the yield and selectivity of CHB (dashed lines, Figs. 5B and 6B). A slight increase in the formation of BCH was observed in the second stage, because the yield and the selectivity of BCH increased, while those of HH-DBT decreased (dashed lines, Figs. 5B and 6B).

3.4. HDS of HH-DBT

HH-DBT reacted fast and its conversion reached 97% at τ = 1.5 g min/mol (solid line, Fig. 7A). CHB was the main product and its yield increased with weight time. Besides TH-DBT, CHB,

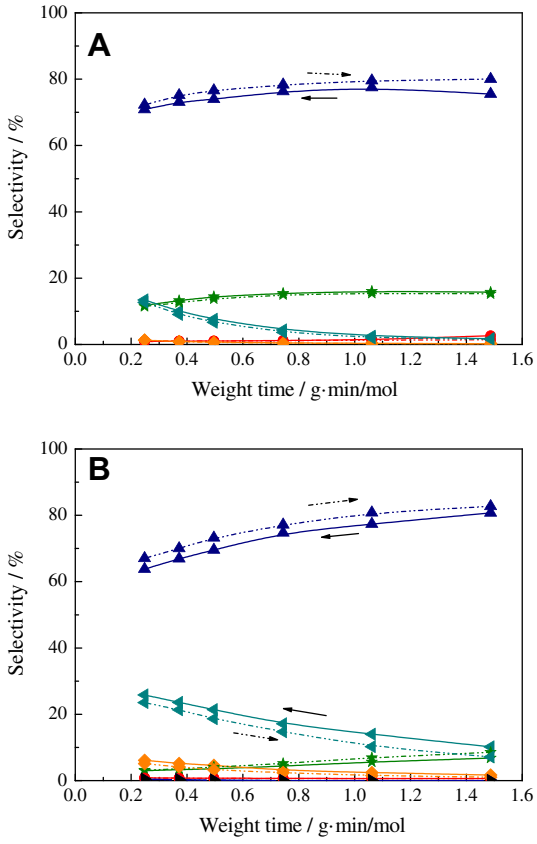

Fig. 6. Product selectivities in the HDS of TH-DBT over bulk MoP at 340 °C and 0 kPa Pi (A) and 0.25 kPa Pi (B) as a function of weight time. ● BP; ▲ CHB; ★ BCH; ◄ HH-DBT; ♦ CHEB-1; ► CHEB-3. The arrows indicate whether the weight time was increased or decreased.

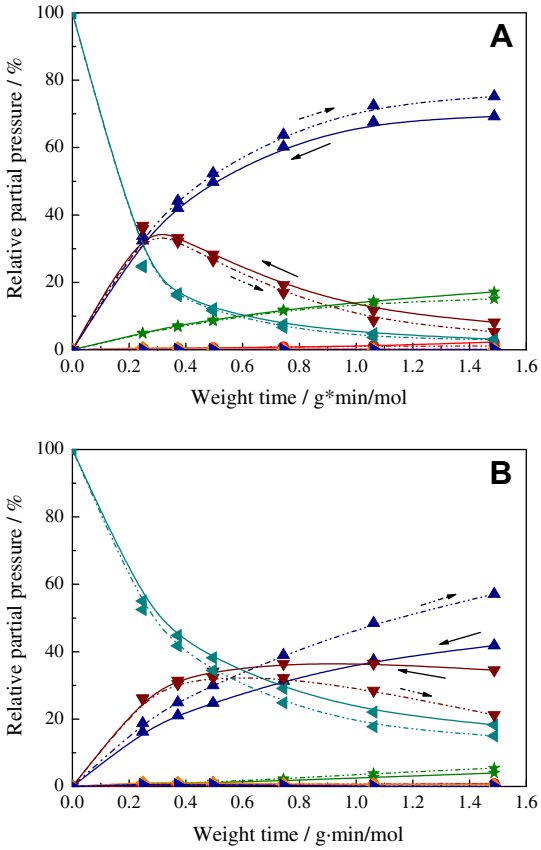

Fig. 7. Relative partial pressures of the reactant and products in the HDS of HH-DBT over bulk MoP at 340 °C and 0 kPa Pi (A) and 0.25 kPa Pi (B) as a function of weight time. ● BP; ▲ CHB; ★ BCH; ▼ TH-DBT; ◄ HH-DBT; ♦ CHEB-1; ► CHEB-3. The arrows indicate whether the weight time was increased or decreased.

and BCH, small amounts of BP, CHEB-1, and CHEB-3 were detected. TH-DBT was formed by dehydrogenation of the reactant and acted as a primary product because its selectivity decreased with weight time (solid line, Fig. 8). Its yield passed through a maximum (Fig. 7A), indicating that further reaction (i.e., desulfurization) occurred. TH-DBT and HH-DBT tended to equilibrium, with a TH-DBT/HH-DBT ratio of 2.6 at $\tau = 1.5$ g min/mol. The variations of the relative partial pressures of CHB and BCH with weight time were almost the same as those obtained in the HDS of TH-DBT (solid line, Fig. 5A), suggesting that the dehydrogenation/hydrogenation reactions between HH-DBT and TH-DBT are faster than their desulfurization reactions. Because of their formation from HH-DBT as well as TH-DBT, the selectivities of CHB and BCH increased with increasing weight time (solid lines, Fig. 8A). In the second stage of the HDS of HH-DBT, the curve associated with HH-DBT was exactly the same as that in the first stage, but small changes in the product distributions occurred. The yield and selectivity of CHB increased, while those of TH-DBT and BCH decreased (dashed lines, Figs. 7A and 8A).

Pi showed a negative effect on the conversion of HH-DBT. At 0.25 kPa Pi, the conversion of HH-DBT decreased to 82% at $\tau = 1.5$ g min/mol (solid line, Fig. 7B). The formation of CHB and BCH was much more inhibited than the conversion of HH-DBT, leading to a significant increase in the yield and selectivity of TH-DBT, the dehydrogenation product and desulfurization intermediate of the HDS of HH-DBT (solid lines, Figs. 7B and 8B). Instead of CHB, TH-DBT became the main product at $\tau < 1.0$ g min/mol (solid lines, Figs. 7B and 8B). In the presence of Pi, the formation of CHB was much more enhanced than the conversion of HH-DBT in the second stage of reaction. The increase in its yield and selectivity was accompanied by a significant decrease in the yield and selectivity of TH-DBT (dashed lines, Figs. 7B and 8B). On the other hand, changes in the formation of BCH were negligible compared with the first stage of the HDS of HH-DBT.

4. Discussion

4.1. New active sites

Thiophenic compounds follow pseudo-first-order kinetics [17,33,34] during HDS, and the reaction orders of the total reaction of DBT as well as of the DDS and HYD pathways are one [34]. Since BP is the only product of the DDS pathway and its further reaction is negligible in the presence of sulfur-containing compounds (Fig. S1 in Supplementary material), the selectivity to BP should be independent of the DBT concentration and thus independent of weight time. However, the observed BP selectivity varied with weight time during the first stage of the DBT HDS in the absence of Pi and only became stable in the second stage (Fig. 4A). This suggests that a new active phase, most likely due to the incorporation of sulfur on the surface of MoP as evidenced by the XRF and XPS, is generated during HDS reaction. The negatively charged surface sulfur anions (Fig. 2) must not be attributed to the adsorbed polyaromatic sulfur-containing molecules because the sulfur atoms in a thiophenic-like environment are positively charged and have a binding energy around 164.1 eV [35]. The surface Mo and P species of the spent MoP catalyst were still in the form of molybdenum phosphide. The formation of MoS_2 phase can be excluded because no peak near 229.4 eV in the Mo 3d spectrum of the spent MoP

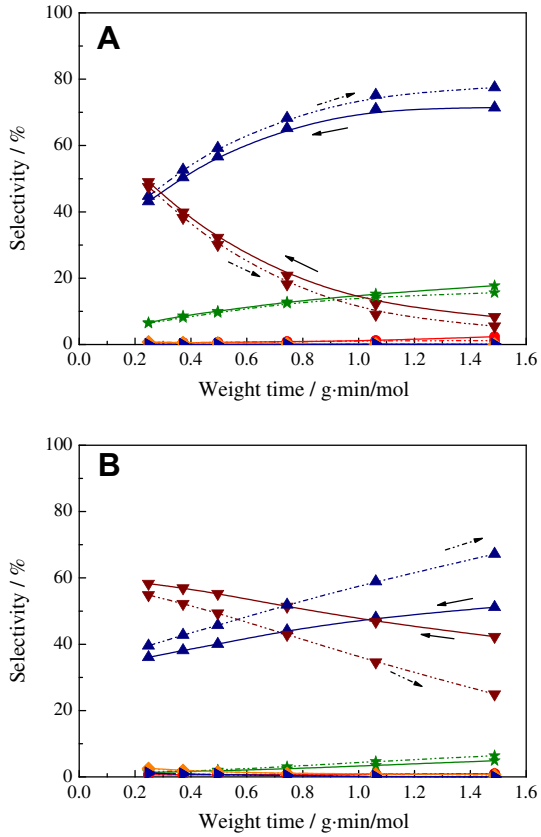

Fig. 8. Product selectivities in the HDS of HH-DBT over bulk MoP at 340 °C and 0 kPa Pi (A) and 0.25 kPa Pi (B) as a function of weight time. ● BP; ▲ CHB; ★ BCH; ▼ TH-DBT; ♦ CHEB-1; ▶ CHEB-3. The arrows indicate whether the weight time was increased or decreased.

catalyst can be detected (Fig. 2). Therefore, this new sulfur-containing phase seems to be a molybdenum phosphosulfide phase (MoP_xS_y).

Sulfur plays an important role in the HDS over transition-metal phosphide hydrotreating catalysts. A nickel phosphosulfide has been established as the real active phase for the working Ni_2P catalysts [6]. The formation of a Ni–S bond on the surface of working Ni_2P catalysts was confirmed by in situ X-ray absorption spectroscopy [36]. Recently, Duan et al. [37] reported that the HDS activity of Ni_2P/MCM-41 correlated well with the sulfur content of the spent catalyst. A DFT calculation indicated the surface with 50% phosphorus replaced by sulfur and some atomic sulfur deposited on the threefold hollow sites was an accurate representation for the actual active phase, or the so-called phosphosulfide surface, of Ni_2P at typical hydrotreating conditions [38]. This may also be the case for MoP. Philips et al. [31] reported that MoP/SiO_2 catalyst displayed an unusual trend of HDS activity that increased monotonically as a function of time on-stream following an initial decline in HDS activity during the first several hours, indicating that the surface of the MoP particles evolved into a more active structure over the course of the activity measurement. Wu et al. found that the initial HDS activity of a MoP/SiO_2 catalyst increased gradually with time in the temperature range from 320 to 400 °C [39], implying that the surface of MoP/SiO_2 undergoes changes under HDS conditions. By studying the adsorption of CO with IR, they found that the surface of MoP/SiO_2 was gradually sulfided under HDS reactions. The change of HDS activity and DDS selectivity with time on-stream was, however, not observed for bulk Ni_2P under the same reaction conditions [23]. This may be due to the different sulfidabilities of MoP and Ni_2P. Sun et al. demonstrated that MoP/SiO_2 can be sulfided by a mixture of thiophene/H_2, whereas more severe sulfiding conditions and a H_2S/H_2 mixture were required to transform Ni_2P/SiO_2 to its phosphosulfide counterpart [40].

In the HDS of TH-DBT and HH-DBT over MoP, the changes in the conversions of TH-DBT and HH-DBT between the first stage and the second stage can only be clearly observed in the presence of Pi. A possible reason is that the HDS of TH-DBT and HH-DBT is much faster than the HDS of DBT, so that the surface sulfidation of MoP is quicker and is already complete in the first stage. Therefore, hardly any change in the catalyst activity in the HDS of TH-DBT and HH-DBT is seen in the absence of Pi (Figs. 5A and 7A). Pi inhibits the HDS reactions and thus the surface sulfidation of the catalyst. As a consequence, the change of the catalytic performance of MoP with time on-stream in the HDS of TH-DBT and HH-DBT became detectable in the presence of Pi. This also suggests that the influence of nitrogen-containing compounds on the HDS activity of MoP is complex. They will not only compete with the sulfur-containing compounds for active sites but also retard the surface sulfidation of MoP. This retarding effect is particularly clear in the HDS of DBT. In the presence of Pi, the selectivity to BP increased but did not reach a constant value (Fig. 4B and Fig. S2 in Supplementary material), indicating that the surface reconstruction of MoP was still in progress even after two reaction stages. It also implies that Pi only slows down the surface sulfidation of MoP but does not react with the MoP surface to yield inactive species. Similar results were reported for Ni_2P/MCM-41. In an investigation in which HDS, HDN, and HDS reactions were alternated, Duan et al. observed that the replacement of sulfur by nitrogen was much faster than that of nitrogen by sulfur [39]. They also observed that in contrast to the O_2-passivated Ni_2P/MCM-41, re-reduction led only to a minor improvement in the HDS performance for the NH_3-passivated catalyst, suggesting that the nitrogen species can hardly be removed by re-reduction or replaced by sulfur species in the course of the HDS reactions. These observations suggest that the inhibition effect of Pi in the HDS of DBT over Ni_2P/MCM-41 is mainly due to its strong adsorption but not to a surface reaction between Pi and the active sites.

In the HDS of DBT, the increase in the DBT conversion between the first and second stage was mainly due to the increase in the yield of BP, the DDS product of DBT HDS, both in the absence and presence of Pi (Fig. 3). For the HDS of TH-DBT and HH-DBT, the decrease in the relative partial pressures of TH-DBT between the first and the second stage was due to the increase in the relative partial pressure of CHB, the DDS product of the HDS of TH-DBT (Figs. 5 and 7). Apparently, the surface sulfidation mainly enhances the DDS activity of MoP. Although the mechanism is not clear, it seems that sulfur atoms or sulfur vacancies on the sulfided surface of MoP catalyst are involved in the extraction of sulfur from the polyaromatic sulfur-containing molecules. For transition-metal sulfides, it has been demonstrated by ^{35}S isotope tracer investigation that sulfur atom exchange between sulfur-containing molecules and the active sites takes place in the HDS reaction [41,42]. The sulfur atoms accommodated on the surface of metal sulfides after HDS could be released only by the introduction of a sulfur-containing compound. To better understand the nature of these new sites and the structure and performance relationship of MoP HDS catalyst, further studies especially the in situ characterizations are needed.

4.2. HDS mechanism

How does the C–S bond breaking in the polyaromatic sulfur-containing compounds occur is still an open question. Hydrogenolysis [43] and elimination [44] are the two mechanisms widely used to describe the cleavage of the C–S bond of the sulfur-containing molecules. According to the hydrogenolysis mechanism, a C–S

bond is broken, and C–H and S–H bonds form simultaneously. Singhal et al. on the other hand proposed that the DDS and HYD pathways had a common dihydro-DBT intermediate [45]. A Hofmann elimination is supposed to be exclusively responsible for the C–S bond breakage of the obtained dihydrogenated product to yield BP [44]. Nine dihydroisomers can be formed through partial hydrogenation of DBT, but only 4,4a-dihydro-DBT and 4a,9b-dihydro-DBT are the two dihydro-intermediates that can undergo DDS by elimination [44]. Unfortunately, these two isomers are kinetically and thermodynamically the least likely ones among the nine dihydro-intermediates [46]. Some recent studied revealed that the desulfurization of the hydrogenated intermediates of DBT and 4,6-DMDBT over transition-metal sulfides may take place by elimination [18,47]. The HDS of DBT and its hydrogenated intermediates over the bulk Ni_2P has been investigated in our previous work [23]. The results suggested that both the hydrogenolysis and elimination mechanism were involved in the DBT HDS reaction network over Ni_2P. DBT and TH-DBT underwent desulfurization mainly through hydrogenolysis to yield BP and CHEB-1, respectively. Due to the relatively low hydrogenation activity of the bulk Ni_2P, the three isomers of cyclohexylbenzene (CHEB-1, CHEB-2, and CHEB-3) were all observed in the HDS product of TH-DBT and HH-DBT. When HH-DBT was the reactant, CHEB-2 was the most abundant cyclohexylbenzene isomer and played a role as one of the primary products. In the separate hydrogenation, CHEB-2 isomerized to CHEB-1 and CHEB-3, but CHEB-1 did not isomerize. This suggested that CHEB-2 was the primary product of the first C–S bond breaking in HH-DBT and that the hydrogen attached to carbon atom C(4) was involved in the HDS over Ni_2P through an β-elimination mechanism.

As shown in Fig. 6, CHEB-1 was a primary product in the HDS of TH-DBT over MoP. The reaction of TH-DBT to CHEB-1 may occur through hydrogenolysis of the C–S bond or by elimination. Direct elimination of H_2S from TH-DBT cannot occur, but a double-bond shift from 1,2,3,4-TH-DBT to 2,3,4,4a-TH-DBT would allow elimination to 2-phenyl-1,3-cyclohexadiene. This diene could then be hydrogenated to CHEB-1 and CHEB-2 [18]. We assume that the double-bond shift and elimination mechanism are less important than the hydrogenolysis mechanism, because no CHEB-2 was detected in the reaction of TH-DBT over MoP. In the present study, only small amounts of CHEB-1 and CHEB-3 were detected in the HDS of HH-DBT over MoP (Fig. 7). Considering the lower CO uptake of bulk MoP (2.2 μmol/g) compared with that of bulk Ni_2P (5.0 μmol/g), this not only indicates that the β-elimination mechanism is valid for the HDS of HH-DBT over MoP, but also suggests that MoP possesses higher hydrogenation activity than Ni_2P. The higher hydrogenation/dehydrogenation activity of MoP is confirmed by the product distribution of the HDS of HH-DBT in the absence of Pi. The yield of TH-DBT already passed through a maximum at low weight time (τ = 0.4 g min/mol) and tended to approach equilibrium with HH-DBT at high weight time (Fig. 7A). On the other hand, in the HDS of HH-DBT over bulk Ni_2P under the same reaction conditions, the yield-time curves indicated that HH-DBT and TH-DBT were far from equilibrium [23]. The BP selectivity (the DDS pathway selectivity) in DBT HDS over Ni_2P was more than 75%, while the value was less than 60% when MoP was used as the catalyst (Fig. 4). This can be another indication to the higher hydrogenation activity of MoP. Small amounts of BP were detected in the HDS of both TH-DBT and HH-DBT over MoP. Similarly, a minor amount of BP was also detected both in the HDS of TH-DBT and HH-DBT as well as in the hydrogenation of CHEB-1 and CHEB-2 over Ni_2P. BP could be the product of the HDS of DBT formed by the dehydrogenation of TH-DBT or HH-DBT. Nevertheless, no DBT was detected in the HDS of TH-DBT and HH-DBT, and the conversion of DBT over the bulk Ni_2P was completely inhibited in the presence of excess of TH-DBT and HH-DBT. Therefore, BP is most likely formed by a disproportionation reaction of CHEBs obtained by the desulfurization of TH-DBT and HH-DBT [23]. This can also be true for MoP, because DBT was not observed in the HDS products of TH-DBT and HH-DBT. Regardless of their different hydrogenation/dehydrogenation performances, the above results and discussion seem to suggest that the reaction network of the HDS of DBT over MoP is similar to that over Ni_2P.

4.3. Kinetics

Since the hydrogenation of CHB to BCH is negligible in the presence of sulfur-containing compounds over MoP (Fig. S1 in Supplementary material), BCH is mainly formed by the hydrogenation of HH-DBT to DH-DBT, which then converts to BCH. No DH-DBT was detected in our experiments, indicating that the desulfurization of DH-DBT to BCH is very fast. Figs. 5 and 7 show that the decrease in TH-DBT concentration in the second stage of the HDS of TH-DBT and HH-DBT over MoP was always accompanied by a similar increase in the yield of CHB, while the yields of the other products for the HDS of TH-DBT were almost unaffected. This indicates that CHB is formed mainly by the desulfurization of TH-DBT, whereas the direct desulfurization of HH-DBT to CHB is slow. We, therefore, propose a reaction network for DBT HDS over MoP as shown in Scheme 1. The reaction constants of each step were calculated from the selectivities of the HDS products of the second reaction stage (the steady state) at short weight time and by assuming pseudo-first-order kinetics. The values are presented in Scheme 1.

The results show that the reaction of HH-DBT to BCH was the slowest step in the network. This must be due to the slow hydrogenation of HH-DBT to DH-DBT, because the desulfurization of DH-DBT is very fast [48]. The second-slowest step, the hydrogenation of DBT to TH-DBT, was about threefold faster than the hydrogenation of HH-DBT to DH-DBT, demonstrating that also over MoP hydrogenation of the second phenyl ring is more difficult than that of the first phenyl ring. This is because the resonance energy of a multi-ring aromatic system is less than that of a mono-aromatic ring. The rate of the DDS of DBT (0.28 mol/g min) was of the same order of magnitude as the rate of hydrogenation of DBT to TH-DBT, in agreement with the comparable DDS and HYD selectivities in the HDS of DBT in the absence of Pi (Fig. 4). Both the hydrogenation of TH-DBT to HH-DBT and the dehydrogenation of HH-DBT to TH-DBT were very fast, the latter being the fastest. These data, along with the reaction profiles of the HDS of TH-DBT and HH-DBT (Figs. 5A and 7A), suggest that these two molecules tended to equilibrium. The desulfurization of TH-DBT to CHB was the second-fastest step. It was about threefold faster than the DDS of DBT and twofold faster than the hydrogenation of TH-DBT to HH-DBT.

The kinetics of the HDS of DBT over MoP is different from those over the bulk Ni_2P and the supported sulfides. Their major differences are briefly summarized below. (1) The direct desulfurization of HH-DBT over MoP was slow, which is different from that over the bulk Ni_2P [23] and sulfided Mo/γ-Al_2O_3 [18] and Ni–Mo/γ-Al_2O_3 [47] but similar to that over Co–Mo/γ-Al_2O_3 sulfide [19]. Over Mo/γ-Al_2O_3 (300 °C, 5 MPa) and Ni–Mo/γ-Al_2O_3 (300 °C, 5 MPa, and in the presence of 35 kPa H_2S) [18,47], the rate constants of desulfurization of HH-DBT to CHB were almost equal to those of TH-DBT to CHB. (2) The ratios of k_{DDS}/k_{HYD} for DBT HDS over Ni_2P (340 °C and total pressure 4 MPa) [23], and the sulfided Mo/γ-Al_2O_3 (300 °C and total pressure 5 MPa) [18], Ni–Mo/γ-Al_2O_3 (300 °C and total pressure 3 MPa) [47], and Co–Mo/γ-Al_2O_3 (300 °C and total pressure 3 MPa) [19] were 4.9, 3.1, 19, and 42, respectively, indicating that the DDS route was much easier than the HYD route for the HDS of DBT over these catalysts. While for MoP, the k_{DDS}/k_{HYD} at 340 °C and 4 MPa was as low as 1.4 (Scheme 1), suggesting that the HYD route was as fast as the

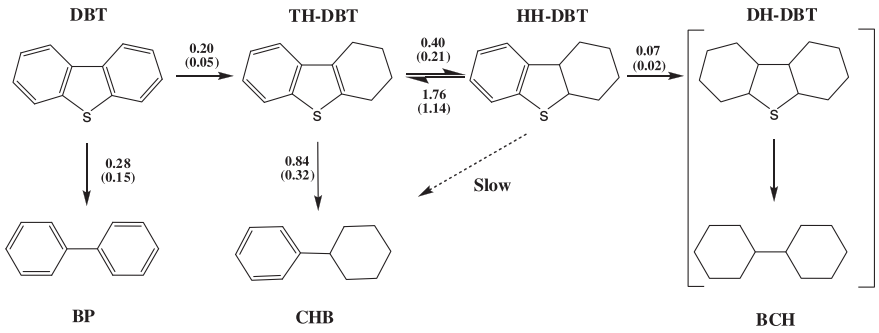

Scheme 1. Pseudo-first-order rate constants (in mol/g min) in the reaction network of the HDS of DBT over MoP at 340 °C and 4 MPa in the absence and presence (in parentheses) of 0.25 kPa Pi.

DDS route. The difference in the kinetic behavior between MoP and the Mo-based sulfides suggests that the nature of the sulfided MoP surface should be different from those of the molybdenum sulfides.

Our results confirm that Pi is a strong poison in the HDS of DBT over MoP. The rate constants of the HYD and DDS pathways were about fourfold lower and twofold lower, respectively, in the presence than in the absence of Pi. This indicates that Pi inhibits both pathways, but the HYD pathway to a greater extent than the DDS pathway. Pi also strongly suppressed the desulfurization of TH-DBT and HH-DBT. However, the reactions between TH-DBT and HH-DBT, especially the dehydrogenation of HH-DBT to TH-DBT, were less affected by Pi. Regardless of this fast interconversion, the HDS of DBT, TH-DBT, and HH-DBT were strongly inhibited by Pi, hydrogenation to a greater extent than desulfurization. This proves that the nitrogen-containing compound adsorbed more strongly than DBT and its partially hydrogenated intermediates on the catalytic sites and adsorbed on both the desulfurization and (de)hydrogenation sites. The degree of inhibition of Pi on the desulfurization of DBT, THDBT, and HHDBT decreased in the order of HHDBT > THDBT > DBT, which can be attributed to the different strengths of adsorption of these molecules on the catalytic sites compared with the nitrogen-containing compound [18].

5. Conclusion

The XRF and XPS results indicated that sulfur was incorporated on the surface of MoP in HDS reactions, probably leading to the formation of new active sites. These new sites had a higher DDS activity than the sites of the fresh MoP catalyst. Both HYD and DDS pathways played an important role in the HDS of DBT over MoP. The hydrogenation of TH-DBT and dehydrogenation of HH-DBT were fast, and these two molecules tended to equilibrium at high weight time. The desulfurization of TH-DBT to CHB was much faster than that of DBT to BP, whereas the reaction of HH-DBT to BCH was the slowest step in the network. HH-DBT mainly desulfurized by dehydrogenation to TH-DBT and subsequent desulfurization of TH-DBT. Pi strongly inhibited the HDS of DBT and its hydrogenated intermediates, hydrogenation more than desulfurization. It not only competed with these sulfur-containing molecules for the adsorption on the active sites but also slowed down the sulfidation of MoP surface.

Acknowledgments

This research was financially supported by the Natural Science Foundation of China (20503003, 20773020, 20973030, and 21073022), the "863" project (2008AA030803), the NCET, the Fundamental Research Funds for the Central Universities, and the "111" project. We are grateful to Prof. Zequn Yin (Fushun Research Institute of Petroleum and Petrochemicals, SINOPEC) for assistance in XPS measurements.

Appendix A. Supplementary material

Supplementary data associated with this article can be found, in the online version, at doi:10.1016/j.jcat.2011.12.018.

References

[1] P. Clark, W. Li, S.T. Oyama, J. Catal. 200 (2001) 140.
[2] S.T. Oyama, P. Clark, X. Wang, T. Shido, Y. Iwasawa, S. Hayashi, J.M. Ramallo-Lopez, F.G. Requejo, J. Phys. Chem. B 106 (2002) 1913.
[3] X. Wang, P. Clark, S.T. Oyama, J. Catal. 208 (2002) 321.
[4] V. Zuzaniuk, R. Prins, J. Catal. 219 (2003) 85.
[5] T. Korányi, Appl. Catal. A Gen. 239 (2003) 253.
[6] S.T. Oyama, J. Catal. 216 (2003) 343.
[7] Y. Kanda, C. Temma, K. Nakata, T. Kobayashi, M. Sugioka, Y. Uemichi, Appl. Catal. A Gen. 386 (2010) 171.
[8] J.R. Hayes, R.H. Bowker, A.F. Gaudette, M.C. Smith, C.E. Moak, C.Y. Nam, T.K. Pratum, M.E. Bussell, J. Catal. 276 (2010) 249.
[9] J.A. Rodriguez, J.Y. Kim, J.C. Hanson, S.J. Sawhill, M.E. Bussell, J. Phys. Chem. B 107 (2003) 6276.
[10] P. Clark, X. Wang, S.T. Oyama, J. Catal. 207 (2002) 256.
[11] S.J. Sawhill, K.A. Layman, D.R. van Wyk, M.H. Engelhard, C. Wang, M.E. Bussell, J. Catal. 231 (2005) 300.
[12] C. Stinner, R. Prins, Th. Weber, J. Catal. 191 (2000) 438.
[13] C. Stinner, R. Prins, Th. Weber, J. Catal. 202 (2001) 187.
[14] R.L. Martin, J.A. Grant, Anal. Chem. 37 (1965) 644.
[15] M. Houalla, N.K. Nag, A.V. Sapre, D.H. Broderick, B.C. Gates, AIChE. J. 24 (1978) 1015.
[16] D.R. Kilanowski, H. Teeuwen, V.H.J. de Beer, B.C. Gates, G.C.A. Schuit, H. Kwart, J. Catal. 55 (1978) 129.
[17] M.J. Girgis, B.C. Gates, Ind. Eng. Chem. Res. 30 (1991) 2021.
[18] H. Wang, R. Prins, J. Catal. 258 (2008) 153.
[19] Y. Sun, R. Prins, J. Catal. 267 (2009) 193.
[20] P. Kukula, V. Gramlich, R. Prins, Helv. Chim. Acta. 89 (2006) 1623.
[21] Y. Sun, H. Wang, R. Prins, Tetrahedron Lett. 49 (2008) 2063.
[22] X. Xu, X. Li, A. Wang, Y. Sun, W.B. Schweizer, R. Prins, Helv. Chim. Acta 94 (2011) 1754.
[23] X. Li, J. Bai, A. Wang, R. Prins, Y. Wang, Top. Catal. 54 (2011) 290.
[24] W. Qian, A. Ishihara, S. Ogawa, T. Kabe, J. Phys. Chem. 98 (1994) 907.
[25] J.C. DiCesare, L.B. Thompson, R.J. Andersen, J. Nail, Org. Prep. Proc. Int. 32 (2000) 169.
[26] Y. Teng, A. Wang, X. Li, J. Xie, Y. Wang, Y. Hu, J. Catal. 266 (2009) 369.
[27] O. Levenspiel, Chemical Reaction Engineering, third ed., Wiley, 1998.
[28] I.I. Abu, K.J. Smith, J. Catal. 241 (2006) 356.
[29] B.V.R. Chowdari, K.L. Tan, F. Ling, Solid State Ionics 113-115 (1998) 711.
[30] H. Al-Kandari, F. Al-Kharafi, A. Katrib, Catal. Commun. 9 (2008) 847.
[31] D.C. Phillips, S.J. Sawhill, R. Self, M.E. Bussell1, J. Catal. 207 (2002) 266.
[32] Z. Mekhalif, F. Sinapi, F. Laffineur, J. Delhalle, J. Electron. Spectrosc. Relat. Phenom. 121 (2001) 149.
[33] M. Egorova, R. Prins, J. Catal. 221 (2004) 11.
[34] Y. Wang, Z. Sun, A. Wang, L. Ruan, M. Lu, J. Ren, X. Li, C. Li, Y. Hu, P. Yao, Ind. Eng. Chem. Res. 43 (2004) 2324.
[35] S.R. Kelemen, G.N. George, M.L. Gorbaty, Fuel 69 (1990) 939.
[36] T. Kawai, K.K. Bando, Y.K. Lee, S.T. Oyama, W.J. Chun, K. Asakura, J. Catal. 241 (2006) 20.
[37] X. Duan, Y. Teng, A. Wang, V.M. Kogan, X. Li, Y. Wang, J. Catal. 261 (2009) 232.
[38] A.E. Nelson, M. Sun, A.S.M. Junaid, J. Catal. 241 (2006) 180.
[39] Z. Wu, F. Sun, W. Wu, Z. Feng, C. Liang, Z. Wei, C. Li, J. Catal. 222 (2004) 41.

[40] F. Sun, W. Wu, Z. Wu, J. Guo, Z. Wei, Y. Yang, Z. Jiang, F. Tian, C. Li, J. Catal. 228 (2004) 298.
[41] A. Wang, Y. Wang, T. Kabe, Y. Chen, A. Ishihara, W. Qian, J. Catal. 199 (2001) 19.
[42] A. Wang, Y. Wang, T. Kabe, Y. Chen, A. Ishihara, W. Qian, P. Yao, J. Catal. 210 (2002) 319.
[43] T. Todorova, R. Prins, Th. Weber, J. Catal. 236 (2005) 190.
[44] F. Bataille, J.L. Lemberton, P. Michaud, G. Pérot, M. Vrinat, M. Lemaire, E. Schulz, M. Breysse, S. Kasztelan, J. Catal. 191 (2000) 409.
[45] G.H. Singhal, R.L. Espino, J.E. Sobel, G.A. Huff Jr., J. Catal. 67 (1981) 457.
[46] M. Egorova, R. Prins, J. Catal. 241 (2006) 162.
[47] H. Wang, R. Prins, J. Catal. 264 (2009) 31.
[48] X. Li, A. Wang, M. Egorova, R. Prins, J. Catal. 250 (2007) 283.